

# Multimodal Speech Enhancement Using Burst Propagation

Leandro A. Passos, Ahmed Khubaib, Mohsin Raza, and Ahsan Adeel  
University of Wolverhampton, Wolverhampton, England, UK  
A.Adeel@wlv.ac.uk

**Abstract**—This paper proposes the MBURST, a novel multimodal solution for audio-visual speech enhancements that consider the most recent neurological discoveries regarding pyramidal cells of the prefrontal cortex and other brain regions. The so-called burst propagation implements several criteria to address the credit assignment problem in a more biologically plausible manner: steering the sign and magnitude of plasticity through feedback, multiplexing the feedback and feedforward information across layers through different weight connections, approximating feedback and feedforward connections, and linearizing the feedback signals. MBURST benefits from such capabilities to learn correlations between the noisy signal and the visual stimuli, thus attributing meaning to the speech by amplifying relevant information and suppressing noise. Experiments conducted over a Grid Corpus and CHiME3-based dataset show that MBURST can reproduce similar mask reconstructions to the multimodal backpropagation-based baseline while demonstrating outstanding energy efficiency management, reducing the neuron firing rates to values up to 70% lower. Such a feature implies more sustainable implementations, suitable and desirable for hearing aids or any other similar embedded systems.

**Index Terms**—Burstpropagation, Multimodal Learning, Audio-Visual Speech Enhancement

## I. INTRODUCTION

The World Health Organization states that 430 million people suffer from moderate to higher hearing loss nowadays and estimates that nearly 2.5 billion will present hearing impairment to some degree by 2050 [1]. The problem impacts the individual social relationships and the perception of surrounding sounds [2], which may also lead to loneliness and psychological distresses [3], [4]. Therefore, intelligent computer systems that boost and clean the audio signal are highly desirable.

In this context, many efforts have been applied toward machine learning-based approaches for speech enhancement [5], [6]. A particularly interesting approach comprises multimodal approaches that combine correlated audio and visual (AV) information to amplify relevant information and suppress noise [7]. The idea can be illustrated by a dialogue in a pub, where people talk and live music is played in the background, and the listener focuses on reading the speaker’s lips and expressions to mind the context and infer meaning from the conversation. The work of Adeel et al. [8] comprises related applications regarding IoT and 5G for lip-reading hearing aids, encrypted audio speech reconstruction [9], and speech enhancement in different conditions using deep learning [10], [11]. Further, the recent work of Passos et al. [12] investi-

gates audio and visual information fusion using Graph Neural Networks and canonical correlation analysis, as well as a cortical cell-inspired model that approximates the computational model to a more biologically plausible approach [13].

Despite such approximation, the methods mentioned above and most of the machine and deep learning solutions rely on backpropagation, an algorithm inspired by an antique modeling of neuronal information flow where inputs are linearly combined and exposed to an activation function, whose output feeds consecutive layers. Further, the outcome is compared to an expected target, and the error is back-propagated, assigning the credit for any mistakes or successes to neurons that are multiple synapses away from the output and updating the weights associated with such neurons accordingly. In this scenario, Payeur [14] proposed a novel approach inspired by more recent studies on the physiological mechanism of pyramidal neurons, where the learning is regulated by the frequency of bursts, the so-called Burstpropagation.

Burstpropagation tackles the credit assignment problem in a more biologically plausible manner by addressing the primary principles of pyramidal neurons suggested by Körding and König [15] as follows. First, it employs a burst-dependent learning rule to steer the sign and magnitude of plasticity through feedback stimuli. Second, it multiplexes the feedback and feedforward information across multiple layers using different connections, i.e., distinct weights are used during the forward and the backward propagation processes. Third, it performs the alignment between feedback and feedforward connections by approximating the loss-function gradients through burst-dependent learning. Finally, the fourth principle regards the linearization of the feedback signals concerning the credit information, which can be performed using recurrent connections.

Therefore, this paper proposes the so-called MBURST, a multimodal approach that combines audio and visual information to enhance speech quality using burst propagation. The model preserves biological properties of real neurons like short-term synaptic plasticity [16], dendritic excitability [17], synaptic transmission, inhibitory microcircuit, and burst-dependent synaptic plasticity [14]. Experiments conducted over a Grid Corpus and CHiME3-based dataset for clean audio mask reconstruction show that MBURST can generate clean audio masks with similar quality to a multimodal backpropagation-based baseline while providing a dramatic reduction in the energy consumption, reaching values up to

70% lower. Such an attribute is extremely desirable for real-world applications like embedded systems on hearing aid devices. Thus, this paper comprises two main contributions:

- it provides the MBURST, a biologically plausible and energy-efficient method that combines audio and visual information for speech enhancement; and
- it introduces burst propagation, a state-of-the-art algorithm inspired by pyramidal neurons, in the context of multimodal learning.

The remainder of this paper is presented as follows. Section II provides a theoretical background regarding Burst-propagation and the proposed approach. Further, Sections III and IV describe the methodology employed to conduct the experiments and the results, respectively. Finally, Section V states the conclusions and future work.

## II. THEORETICAL BACKGROUND

This section briefly introduces the concepts behind burst propagation, as well as the proposed burst propagation-based multimodal approach, namely MBURST.

### A. Burst Propagation

The burst-dependent algorithm, or burst propagation, defines the weighted sum at the neuron’s input as “somatic potentials”. Similarly, the neuron’s output is termed the event rate. The ‘somatic potentials’ of a dense layer are defined as:

$$v_l = W_l e_{l-1}, \quad (1)$$

where  $l \in \{1, 2, \dots, L\}$  denotes the network’s layers,  $W_l$  is the weight connecting layer  $l - 1$  to layer  $l$  and  $e_l$  is the  $l$ th layer’s event rate, defined by:

$$e_l = f(v_l), \quad (2)$$

where  $f_l$  stands for any activation function, e.g., the Rectifier Linear Unit (ReLU) or Sigmoid, for layer  $l$ . Regarding convolution layers, the multiplications are simply replaced by a convolution operator where  $W_l$  represents layer  $l$ ’s kernel.

Since the burst rate drives the model’s learning procedure, the first step in the process comprises computing the output layer ( $l = L$ ) bursting probability:

$$p_L = \zeta(\bar{p}_L - h(e_L) \odot \Delta_{e_L} \mathcal{L}) \quad (3)$$

where  $\bar{p}_L$  is a hyperparameter that defines the reference bursting probability,  $\zeta$  is a squashing function that guarantees  $P_{L,i} \in [0, 1]$ ,  $\Delta_{e_L} \mathcal{L}$  stands for the loss function derivative, and  $h(e_l)$  is a vector-valued function defined by:

$$h(e_l) \equiv f'(v_l) \odot e_l^{-1}. \quad (4)$$

The bursting probability is used to calculate the bursting rate with and without teaching, i.e.,  $b_l$  and  $\bar{b}_l$ , respectively, at any layer  $l$ :

$$\begin{aligned} b_l &= p_l \odot e_l, \\ \bar{b}_l &= \bar{p}_l \odot e_l. \end{aligned} \quad (5)$$

Further, the bursting rates are propagated to the previous layers through feedback weights, namely  $Y$ . The result is employed to compute the current hidden layer’s “dendritic potential” with ( $u_l$ ) and without ( $\bar{u}_l$ ) teacher. Notice that, for convolutional layers,  $Y$  stands for a kernel, and a convolution operation replaces the multiplication.

$$\begin{aligned} u_l &= h(e_l) \odot (Y_l b_{l+1}), \\ \bar{u}_l &= h(e_l) \odot (Y_l \bar{b}_{l+1}). \end{aligned} \quad (6)$$

In the sequence, the somatic potentials are used to calculate the hidden layer’s bursting probability and the reference bursting probability:

$$\begin{aligned} p_l &= \sigma(\beta u_l + \alpha), \\ \bar{p}_l &= \sigma(\beta \bar{u}_l + \alpha), \end{aligned} \quad (7)$$

where  $\beta = 1$  and  $\alpha = 0$  are constants that control the dendritic transfer function and  $\sigma$  is a sigmoid function.

Finally, the change in the forward and feedback weights,  $W$  and  $Y$ , respectively, are computed as follows:

$$\Delta W_l = \Delta Y_l = -(b_l - \bar{b}_l) \odot e_{l-1}^T. \quad (8)$$

Notice that, once again, the multiplication is replaced by a backward convolution in the context of convolutional layers.

### B. MBURST

The proposed multimodal burst propagation-based approach to speech enhancement combines audio and visual information for clean audio estimation. The model takes advantage of recent neurological research on pyramidal cells to learn coherent relationships between noisy audio and visual information and extract clean information by amplifying relevant information and suppressing noise.

The model comprises two burst-dependent convolutional neural networks that work in parallel to extract features from noisy audio inputs and their respective frames. The outcomes from both channels are flattened and exposed to a burst-dependent fully-connected layer for embedding extraction. The embeddings are concatenated into a single feature vector, which is used to feed a similar burst-dependent dense layer for classification. Figure 1 depicts the process pipeline.

## III. METHODOLOGY

This section describes the dataset and the environment configuration considered in the experiments.

### A. Dataset

The experiments performed in this work were conducted over a dataset based on roughly 1,000 sentences composed of a six-word sequence extracted from Speakers 1 in Grid Corpus [18] dataset. The clear Grid utterances are blended with non-stationary random noises, e.g., bus, cafe, street, and pedestrian, using four distinct Signal-to-noise ratios (SNR), i.e.,  $\{-12dB, -6dB, 0dB, 6dB\}$ , extracted from the 3rd CHiME Challenge (CHiME3)[19].

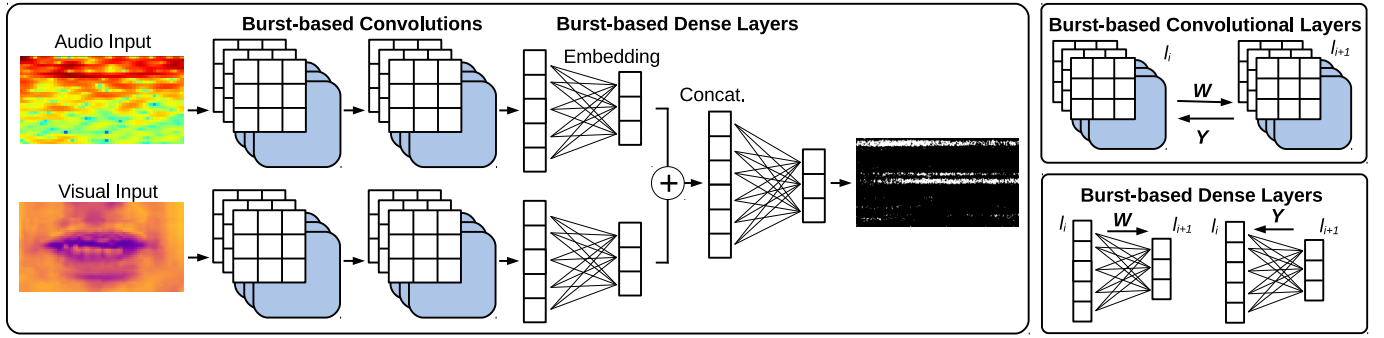


Fig. 1. Proposed method. The left image depicts the multimodal network with noisy audio and visual inputs. Both channels comprise two layers of burst-based convolutions, followed by flattening and a burst-based dense layer for feature embedding. Finally, such embeddings are concatenated and used to feed another burst-based dense for classification. Right-top and right-bottom frames illustrate the burst-based convolutional and dense layers, respectively. Notice such layers comprise a forward weight matrix (kernel)  $W$  and a backward weight matrix  $Y$ .

1) *Data pre-processing*: The original audio was resampled at 16 kHz. Each utterance was divided into approximately 75 frames with 1,244 samples per frame and a 25% increment rate. Further, a 622-bin power spectrum was computed using STFTs and a hamming window procedure. A Viola-Jones lip detector [20] and an object tracker [21] extract the speakers' lip images from the GRID Corpus films, recorded at 25 frames per second. A  $92 \times 50$ -inch area around the lip's center was picked. The recovered lip sequences were up-sampled three times to match the 75 STFT frames of the audio signal.

2) *Ideal Binary Mask*: Hu and Wang [22] proposed the so-called Ideal Binary Mask (IBM), a binary mask with a positive value to a time-frequency (TF) unity whose goal energy is greater than the interference energy and zero otherwise. Among a number of the desired qualities in speech enhancement, the binary masks retain the speech-dominated units while zeroing out the noise-dominated units of noisy speech and providing high intelligibility scores on speech reconstruction, even considering meager signal-to-noise ratio (SNR) settings [23].

IBM employs a premixing of target and interference signals, i.e., the speech and noise signals, computed through a criterion function:

$$IBM(t, f) = \begin{cases} 1 & \text{if } 10 \log_{10} \left( \frac{X(t, f)^2}{N(t, f)^2} \right) \geq LC, \\ 0 & \text{otherwise} \end{cases} \quad (9)$$

where  $X$  stands for the speech with no background noise,  $N$  represents the noise portion, and  $LC$  is the local criterion used to differentiate between speech and background noise, i.e., a threshold. Further, the frame of reference  $t$  and the frequency range  $f$  denote the time and frequency dimensions, respectively.

The method assigns a positive value to the more prevalent TF units if their SNR is greater than or equal to the LC. Conversely, TF units dominated by noise are presumed to have SNRs lower than LC. Thus they are given assigned a value of 0 and muted. The proportion of the TF-positive speech versus noise-dominant samplings relies on a proper LC selection. Since SNRs greater than 0 dB are speech dominating and those

less than 0 dB are noise dominant, an LC of 0 dB is supposedly optimal. However, studies suggest that such selection may imply disproportionate removal of TF units on mixed noisy and speech instances due to the addition of noise known as artifacts, therefore suggesting employing an LC of 5 dB [24], [24] for optimum performance.

### B. Experimental Setup

This work implements MBURST, a burst propagation-based multimodal architecture for speech enhancement. The architecture comprises two parallel networks, i.e., an audio and a visual channel, each containing two convolutional layers with 32 channels, followed by flattening and a dense layer with 256 units for embedding extraction. Finally, such embeddings are concatenated and used to feed the top layer, which is encharged to estimate the clean audio masks. It also implements two baselines for comparison purposes, i.e., a similar network using the same configuration but the backpropagation algorithm for learning, namely Multimodal and a unimodal version also trained using backpropagation that comprises the same architecture except by the visual channel, namely unimodal.

The convolutions consider kernels of size  $3 \times 3$ , paddings equal to 1, and a stride of size 2 for the visual and 1 for the audio channels. This difference in the stride concerns the shape of the audio input, i.e., since the input audio comprises the current signal, composed of 500 features, plus the seven prior frames, forming an  $8 \times 500$  matrix, we opted to use stride 1 to maintain this shape due to the reduced size.

The experiments were conducted using the weighted binary cross entropy as the loss function since the rate of white pixels in the masks (relevant information) is several times smaller than black ones. The same justificative is considered for employing the F1-score as the evaluation metric. Further, the optimization of the parameters is conducted using Adam with a learning rate of  $10^{-3}$  and weight decay of  $10^{-6}$ . Regarding burst propagation, the reference bursting probability follows the standard value adopted by the original work [14], setting  $\bar{P}_L = 0.2$ . The dataset was randomly split into training (80%), testing (15%), and proxy (5%) sets. The training is

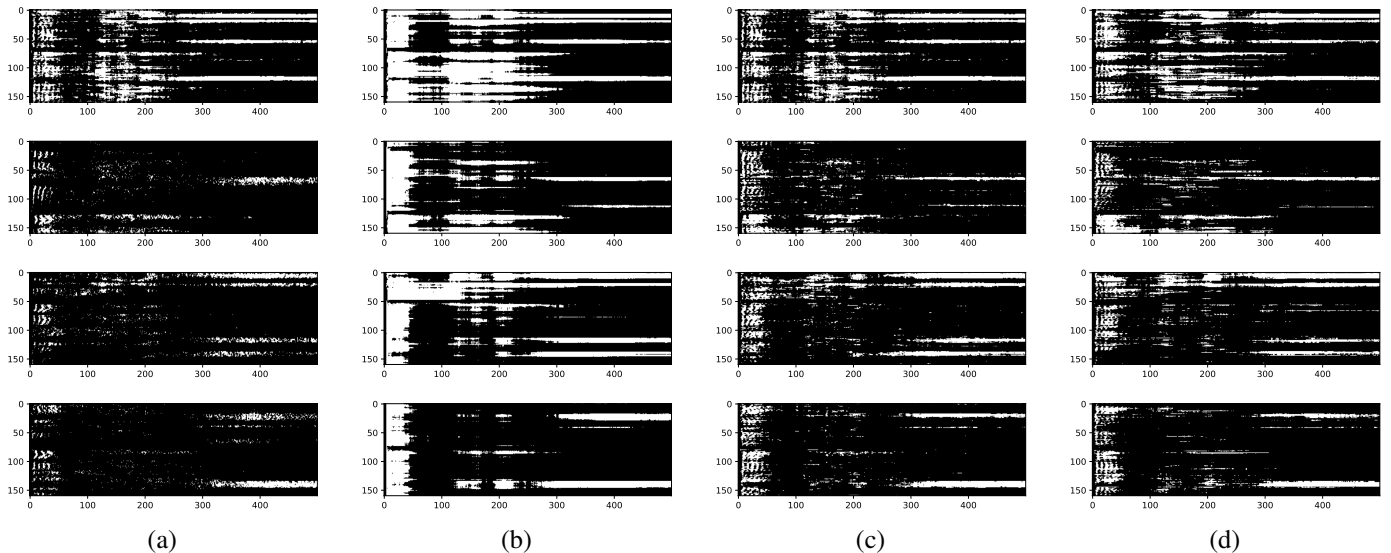


Fig. 2. Multimodal-based mask reconstructions: (a) Original mask, (b) reconstruction using Unimodal, (c) Multimodal, and (d) the proposed MBURST.

conducted for 4 runs, considering different dataset splits, during 40 epochs.

Finally, MBURST, as well as the baseline architectures, were implemented in Python using Pytorch framework [25], and the code is available on GitHub<sup>1</sup>.

#### IV. EXPERIMENTAL RESULTS

This section presents the results and discussion under the perspectives of clean audio signal mask reconstruction and energy efficiency.

##### A. Clean Audio Signal Mask Reconstruction

Table I presents the average F1-score and accuracy, as well as their respective standard deviations, over the training and test sets for the proposed MBURST and the baseline architectures. In this scenario, one can notice that the Unimodal was not capable of providing competitive results, which is expected since the visual context is essential to introduce context to the noisy signal and boost the reconstruction. On the other hand, both the Multimodal and MBURST obtained similar results, with the Multimodal approach achieving slightly better values (less than 2% on average), which can be possibly explained by activation sparsity induced by the burst rate mechanism. Such results reinforce the relevance of visual context for clean speech reconstruction.

Figure 2 depict some examples of the reconstructions themselves. Notice that such images were generated by gathering groups of 150 randomly selected sequential samples from the proxy data set. In this context, one can observe that the masks reflect the results provided in Table I, i.e., Unimodal presents a poor mask reconstruction, while both the Multimodal and the MBURST provide more accurate and very similar results. Once again, the results suggest that correlated visual context is essential to extract more relevant information from noisy audio signals and improve the reconstruction quality.

<sup>1</sup>Available at: <https://github.com/Leandropassosjr/MBURST>.

TABLE I  
F1-SCORE AND ACCURACY CONCERNING THE UNIMODAL, MULTIMODAL, AND THE PROPOSED MBURST FOR CLEAN AUDIO MASK RECONSTRUCTION OVER THE TRAIN AND TEST SETS.

Data set	Metric	Unimodal	Multimodal	MBURST
<b>Train</b>	F1	$0.677 \pm 0.000$	$0.802 \pm 0.005$	$0.782 \pm 0.001$
	Acc.	$82.919 \pm 0.043$	$91.898 \pm 0.220$	$90.602 \pm 0.067$
<b>Test</b>	F1	$0.696 \pm 0.000$	$0.790 \pm 0.003$	$0.768 \pm 0.002$
	Acc.	$81.758 \pm 0.047$	$90.236 \pm 0.164$	$88.798 \pm 0.233$

##### B. Energy Analysis

This work considers the energy efficiency in terms of neurons' activation rate, which shows itself as MBURST's major triumph. In this aspect, one can observe in Figure 3 that the MBURST neurons' firing rate decreases dramatically to values below 0.2 in the first iterations and strides towards values close to 0.1 in the subsequent iterations for both training and testing sets, showing an energy gain around 70% and 65% over the Multimodal and Unimodal approaches, respectively. Regarding the backpropagation-based approaches, the Unimodal performed better than Multimodal, suggesting that the backpropagation was not robust enough to combine the noisy audio and visual information in an energy efficiency fashion, thus implying the worst performance achieved by the Multimodal approach in this context.

Table II analytically reinforces MBURST's robustness in the context of energy efficiency by presenting the area under the curve over the average energy rate measured during the training and testing procedures. In this context, MBURST shows itself 48% and 58%, on average over train and test sets, more efficient than Unimodal and Multimodal, respectively.

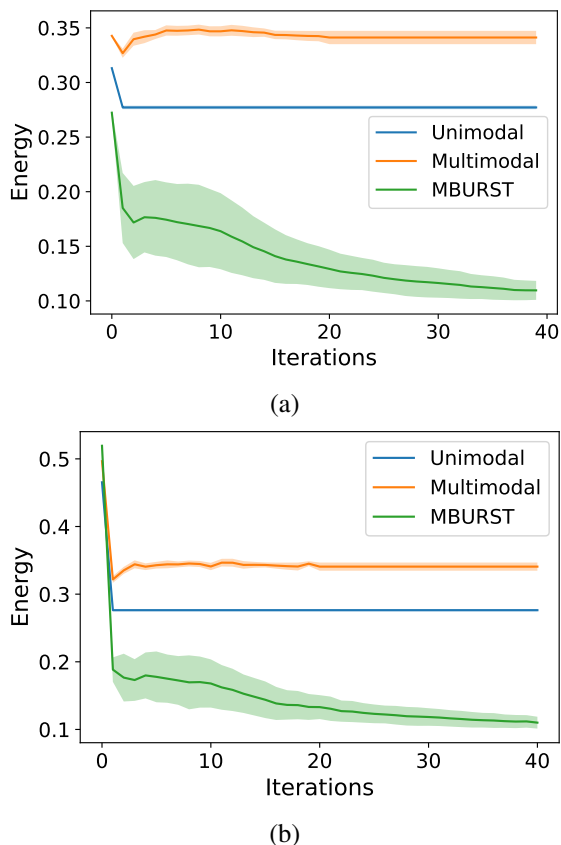


Fig. 3. Energy efficiency rate over (a) train and (b) test sets.

TABLE II  
AREA UNDER THE CURVE CONSIDERING THE AVERAGE ENERGY RATE DURING TRAINING AND TESTING FOR THE UNIMODAL, MULTIMODAL, AND THE PROPOSED MBURST.

Data set	Unimodal	Multimodal	MBURST
<b>Train</b>	11.12	13.70	5.63
<b>Test</b>	11.51	14.14	6.08

## V. CONCLUSIONS

This paper proposed the MBURST, a burst propagation-based multimodal approach that implements a more biologically plausible solution for the task of AV speech enhancement. One can draw two main conclusions from experiments conducted over a Grid Corpus and CHiME3-based dataset. First, multimodal AV architectures are more efficient than a standard unimodal approach for clean audio mask reconstruction since correlated visual information provides contextual meaning to noisy audio. Second, MBURST can produce similar results to a traditional backpropagation multimodal architecture in the context of accuracy and reconstruction task metrics, with a massive advantage regarding energy efficiency due to the burst-rate-based activation mechanism.

Regarding future work, we aim to extend the burst propagation concepts to recent studies comprising context-sensitive

neocortical neurons [26] and canonical cortical networks [13].

## ACKNOWLEDGMENTS

The authors are grateful to the Engineering and Physical Sciences Research Council (EPSRC) grant EP/T021063/1.

## REFERENCES

- [1] W. H. Organization *et al.*, “Hearing screening: considerations for implementation,” 2021.
- [2] W. Noble, *Self-assessment of hearing and related function*. Wiley-Blackwell, 1998.
- [3] A. R. Huang, J. A. Deal, G. W. Rebok, J. M. Pinto, L. Waite, and F. R. Lin, “Hearing impairment and loneliness in older adults in the united states,” *Journal of Applied Gerontology*, vol. 40, no. 10, pp. 1366–1371, 2021.
- [4] A.-S. Helvik, G. Jacobsen, and L. R. Hallberg, “Psychological well-being of adults with acquired hearing impairment,” *Disability and rehabilitation*, vol. 28, no. 9, pp. 535–545, 2006.
- [5] N. Das, S. Chakraborty, J. Chaki, N. Padhy, and N. Dey, “Fundamentals, present and future perspectives of speech enhancement,” *International Journal of Speech Technology*, vol. 24, no. 4, pp. 883–901, 2021.
- [6] R. Rehr and T. Gerkmann, “On the importance of super-gaussian speech priors for machine-learning based speech enhancement,” *IEEE/ACM Transactions on Audio, Speech, and Language Processing*, vol. 26, no. 2, pp. 357–366, 2017.
- [7] J. Ngiam, A. Khosla, M. Kim, J. Nam, H. Lee, and A. Y. Ng, “Multimodal deep learning,” in *ICML*, 2011.
- [8] A. Adeel, J. Ahmad, and A. Hussain, “Real-time lightweight chaotic encryption for 5g iot enabled lip-reading driven secure hearing-aid,” *arXiv preprint arXiv:1809.04966*, 2018.
- [9] A. Adeel, J. Ahmad, H. Larijani, and A. Hussain, “A novel real-time, lightweight chaotic-encryption scheme for next-generation audio-visual hearing aids,” *Cognitive Computation*, vol. 12, no. 3, pp. 589–601, 2020.
- [10] A. Adeel, M. Gogate, and A. Hussain, “Contextual deep learning-based audio-visual switching for speech enhancement in real-world environments,” *Information Fusion*, vol. 59, pp. 163–170, 2020.
- [11] M. Gogate, K. Dashtipour, A. Adeel, and A. Hussain, “Cochleanet: A robust language-independent audio-visual model for real-time speech enhancement,” *Information Fusion*, vol. 63, pp. 273–285, 2020.
- [12] L. A. Passos, J. P. Papa, J. Del Ser, A. Hussain, and A. Adeel, “Multimodal audio-visual information fusion using canonical-correlated graph neural network for energy-efficient speech enhancement,” 2022. [Online]. Available: <https://arxiv.org/abs/2202.04528>
- [13] L. A. Passos, J. P. Papa, and A. Adeel, “Canonical cortical graph neural networks and its application for speech enhancement in future audio-visual hearing aids,” *arXiv preprint arXiv:2206.02671*, 2022.
- [14] A. Payeur, J. Guerguiev, F. Zenke, B. A. Richards, and R. Naud, “Burst-dependent synaptic plasticity can coordinate learning in hierarchical circuits,” *Nature neuroscience*, vol. 24, no. 7, pp. 1010–1019, 2021.
- [15] K. P. Körding and P. König, “Supervised and unsupervised learning with two sites of synaptic integration,” *Journal of computational neuroscience*, vol. 11, no. 3, pp. 207–215, 2001.
- [16] H. Markram, Y. Wang, and M. Tsodyks, “Differential signaling via the same axon of neocortical pyramidal neurons,” *Proceedings of the National Academy of Sciences*, vol. 95, no. 9, pp. 5323–5328, 1998.
- [17] M. E. Larkum, J. J. Zhu, and B. Sakmann, “A new cellular mechanism for coupling inputs arriving at different cortical layers,” *Nature*, vol. 398, no. 6725, pp. 338–341, 1999.
- [18] M. Cooke, J. Barker, S. Cunningham, and X. Shao, “An audio-visual corpus for speech perception and automatic speech recognition,” *The Journal of the Acoustical Society of America*, vol. 120, no. 5, pp. 2421–2424, 2006.
- [19] J. Barker, R. Marxer, E. Vincent, and S. Watanabe, “The third ‘chime’ speech separation and recognition challenge: Analysis and outcomes,” *Computer Speech & Language*, vol. 46, pp. 605–626, 2017.
- [20] P. Viola and M. Jones, “Rapid object detection using a boosted cascade of simple features,” in *Proceedings of the 2001 IEEE computer society conference on computer vision and pattern recognition. CVPR 2001*, vol. 1. Ieee, 2001, pp. I–I.
- [21] D. A. Ross, J. Lim, R.-S. Lin, and M.-H. Yang, “Incremental learning for robust visual tracking,” *International journal of computer vision*, vol. 77, no. 1, pp. 125–141, 2008.

- [22] G. Hu and D. Wang, "Monaural speech segregation based on pitch tracking and amplitude modulation," *IEEE Transactions on neural networks*, vol. 15, no. 5, pp. 1135–1150, 2004.
- [23] Y. Jiang, H. Zhou, and Z. Feng, "Performance analysis of ideal binary masks in speech enhancement," in *2011 4th International Congress on Image and Signal Processing*, vol. 5. IEEE, 2011, pp. 2422–2425.
- [24] E. W. Healy, S. E. Yoho, J. Chen, Y. Wang, and D. Wang, "An algorithm to increase speech intelligibility for hearing-impaired listeners in novel segments of the same noise type," *The Journal of the Acoustical Society of America*, vol. 138, no. 3, pp. 1660–1669, 2015.
- [25] A. Paszke, S. Gross, F. Massa, A. Lerer, J. Bradbury, G. Chanan, T. Killeen, Z. Lin, N. Gimelshein, L. Antiga, A. Desmaison, A. Kopf, E. Yang, Z. DeVito, M. Raison, A. Tejani, S. Chilamkurthy, B. Steiner, L. Fang, J. Bai, and S. Chintala, "Pytorch: An imperative style, high-performance deep learning library," in *Advances in Neural Information Processing Systems 32*. Curran Associates, Inc., 2019, pp. 8024–8035. [Online]. Available: <http://papers.neurips.cc/paper/9015-pytorch-an-imperative-style-high-performance-deep-learning-library.pdf>
- [26] A. Adeel, M. Franco, M. Raza, and K. Ahmed, "Context-sensitive neocortical neurons transform the effectiveness and efficiency of neural information processing," *arXiv preprint arXiv:2207.07338*, 2022.